Development of Paramagnetic Probes for Molecular Recognition Studies in Protein Kinases

Jesus Vazquez, **Surya K. De**, **Li-Hsing Chen**, **Megan Riel-Mehan**, **Aras Emdadi**, **Jason Cellitti**, **John L. Stebbins**, **Michele F. Rega**, and **Maurizio Pellecchia**[*]
Burnham Institute for Medical Research, La Jolla, California

Abstract

We report on the synthesis and evaluation of an indazole-spin-labeled compound that was designed as an effective chemical probe for second site screening against the protein kinase JNK using NMR-based techniques. We demonstrate the utility of the derived compound in detecting and characterizing binding events at the protein kinase docking site. In addition, we report on the NMR-based design and synthesis of a bidentate compound spanning both the ATP site and the docking site. We show that the resulting compound has nanomolar affinity for JNK despite the relatively weak affinities of the individual fragments that constitute it. The approach demonstrates that targeting the docking site of protein kinases represents a valuable yet unexplored avenue to obtain potent kinase inhibitors with increased selectivity.

Introduction

JNKs are a family of serine/threonine protein kinases members of the superfamily of the mitogen-activated protein kinases (MAPK).[a] Misregulation of JNK activation results in several human disorders.[1] JNK is associated to inflammatory diseases modulating TNF-α secretion among other proteins,[2,3] neurodegenerative diseases, where JNK activity is correlated to neuronal apoptosis,[4,5] metabolic diseases, where JNK inhibits insulin signaling,[6,7] and cancer, where several tumor cell lines have been reported to possess active JNK.[8-10] JNKs are therefore very promising drug targets for the development of novel therapies against a variety of diseases.

There are three JNK genes in mammals encoding JNK-1, JNK-2, and JNK-3 proteins, which are very similar in structure and composition to each other. JNK binds to scaffold proteins and substrates containing a D-domain, which *consensus* sequence is R/KXXXXLXL.[11,12] JNK-

[a]Abbreviations:

JNK	C-Jun N-terminal protein kinase
MAPK	mitogen-activated protein kinases
JIP1	JNK-interacting protein-1
ILOE	interligand Overhauser effect
TEMPO	2,2,6,6-tetramethylpiperidine 1-oxyl
WSC	water soluble carbodiimide
DELFIA	dissociation-enhanced lanthanide fluorescent immunoassay

interacting protein-1 (JIP1) is a scaffolding protein that enhances JNK signaling by creating a proximity effect between JNK and upstream kinases.[13] The JNK–JIP1 interaction is mediated by a specific, high affinity D-domain on JIP1. The overexpression of either the D-domain of JIP1 or the full-length protein potently inhibits JNK signaling in the cell. The minimal region of JIP1 consisting in the single D-domain has been identified as retaining the JNK-inhibitory property.[14-16] This peptide, pepJIP1 (a peptide of sequence RPKRPTTLNLF corresponding to the D-domain of JIP1), inhibited JNK activity in vitro toward recombinant c-Jun, Elk, and ATF2 and displayed a remarkable selectivity (no inhibition of the closely related Erk and p38 MAPKs).[17]

The recently determined X-ray structure of JNK1 in complex with pepJIP1 and the ATP-mimic SP600125 (**1**)[17,18] reveals a close proximity between the ATP and the JIP1 binding sites, suggesting the possibility to obtain high affinity and selective compounds by designing appropriate bidentate molecules. Hence, our hypothesis is that by tailoring a second-site JIP1-mimic to an ATP-mimic, it should be possible to develop potent and selective inhibitors of the therapeutically relevant JNK and potentially to other MAPKs that contain specific docking sites.

An interesting approach to screen for second site binders was recently reported by Jahnke and co-workers.[19-21] This method utilizes initial binders chemically labeled with organic nitroxide radicals ("spin labels" such as the 2,2,6,6-tetramethylpiperidine 1-oxyl (TEMPO)) to perform second-site NMR spectroscopic screens of fragment libraries. The binding of a second-site ligand can be simply detected by measuring the relaxation enhancement induced by the spin-labeled first ligand.[19-21] We also recently reported the use of furanyl-salicyl-nitroxide derivatives as versatile probes for NMR-based second-site screening in protein tyrosine phosphatases.[22]

Such chemical tools are then useful for the design and synthesis of bidentate compounds with increased affinity but also specificity for a given target. In fact, if specificity is a major issue, second site ligands that are specific for a given protein may be selected by performing the NMR screening against counter targets. On the basis of these premises, we report herein the synthesis and characterization of the indazole-nitroxide derivative **9** (Figure 1), its use as a probe for structural determination of docking-site binders, and the NMR-based design of the very first bidentate, substrate competitive inhibitor of JNK (Figure 2).

Results and Discussion

The design of the paramagnetic probe was based on the structure of the ATP-mimic **1** (Figure 1A),[17,18] but in which the keto group was removed to facilitate the subsequent synthetic efforts (Figure 1B). The X-ray structure of the ternary complex between JNK1, compound **1**, and a JIP1 peptide[18] suggests the most convenient position to elongate the ATP mimic toward the JIP1 site (Figure 1A,B). The length and nature of the linker were investigated by molecular modeling studies, leading to the design of compound **9**, which is predicted to bring the unpaired electron of the TEMPO just at the edge of the JIP1 binding site (Figure 1A).

Thus, the synthesis of compound **9** starts from the 1-azaindole (Figure 1B). After the iodination of the 1-azaindole with iodide and its protection with *tert*-butyloxy anhydride, a Suzuki coupling between **4** and 4-methoxycarbonylphenylboronic acid yielded compound **5**. This compound was then saponificated with lithium hydroxide and the Boc group was sequentially eliminated in presence of 3N HCl.

An amide bond was formed between the resulting compound **6** and the methyl 4-aminobutanoate, obtaining compound **7** with a 62% yield. The ester was then saponificated

with lithium hydroxide. The free acid **8** was used to anchor the 4-amino TEMPO through an amide bond employing water-soluble carbodiimide (WSC).

To characterize the affinity of the compounds, we tested their inhibitory activity against JNK. The paramagnetic compound **9** showed an inhibition constant of 1.2 μM. Compound **8**, which lacks the 4-amino TEMPO attached, had an IC_{50} of 1.4 μM, showing that the addition of the paramagnetic moiety does not affect the inhibitory properties of the indazole derivative. Subsequently, we monitored the effect of the paramagnetic compound on the NMR spectra of pepJIP1 or its fragments. The peptides we used were Ac-RPTTLNL-OH and Ac-LNL-OH. The affinities of these peptides for JNK were determined by employing a displacement assay based on the DELFIA (dissociation-enhanced lanthanide fluorescent immunoassay) platform in which a biotin-linked pepJIP1 is adsorbed onto a streptavidin-coated plate followed by incubation with GST-JNK1. Detection of the pep-JIP1/GST-JNK complex is facilitated by a highly fluorescent anti-GST Eu-antibody conjugate (Perkin-Elmer). In this assay, the peptide Ac-RPTTLNL-OH showed an IC_{50} of 53 μM, whereas the peptide Ac-LNL-OH had no appreciable displacement up to 200 μM. These values are in good agreement with the JNK inhibition studies previously reported for pepJIP1 and related peptides.[11,12] Subsequently, we recorded ^{1}H NMR $T_{1\rho}$ experiments with these peptides in the presence of JNK and in presence and absence of the paramagnetic probe **9**. When the paramagnetic probe was in the sample mixture, the proton NMR signals of both peptides are largely attenuated in these experiments (Figures 1C and 2A) due to their proximity to the unpaired electron of compound **9**. The unpaired electron possesses a gyromagnetic ratio 657 times higher than a hydrogen nucleus and thus produces a very efficient distance-dependent relaxation effect via dipole–dipole interactions with a given nucleus. This observation has two important implications. First, only compounds that bind to JNK at the JIP1 site will experience the relaxation enhancement effect of the paramagnetic probe. Second, analysis of the differential signal reduction within the test molecule provides crude but significant information on the relative orientation of such a molecule with respect to the indazole–TEMPO compound. Accordingly, in examining the signal intensity reduction induced by the indazole–TEMPO on the pepJIP peptides, it is evident that the various residues experience different relaxation enhancement effects (Figures 1C and 2A). For the peptide Ac-RPTTLNL-OH, the C-terminal leucine is the most affected residue, being the closest to the unpaired electron of TEMPO, while the acetylated N-terminal arginine is the less affected one, being the most distant from the paramagnetic probe (Figure 1D). Furthermore, by monitoring the displacement of the signal reduction of a known reference molecule (the pepJIP1 for example) by a test compound, it is possible to estimate its inhibitory constant (Supporting Information).[23] Again, these data suggest that compound **9** can be used to characterize binding and to rapidly gather structural information about the relative orientation of a test molecule in the bound state, which constitutes fundamental information for the design of bidentate inhibitors.

One advantage of the fragment-based approach is that the covalent linkage of even weakly interacting fragments can lead to high affinity compounds.[24-27] To illustrate the usefulness of compound **9** in such endeavors, we report on the synthesis and characterization of compound **12**.

The tripeptide Ac-LNL-OH has no appreciable displacement up to 200 μM in the DELFIA assay. However, it binds weakly in the JIP pocket as evident by the NMR data in the presence of the paramagnetic probe **9** (Figure 2), suggesting that it can be a suitable fragment for the design of a higher affinity compound when tethered with the ATP-mimic. The design of a proper linker between Ac-LNL-OH and the indazole derivative was determined based on the paramagnetic compound **9** and the differential relaxation effect it induced on the tripeptide. Two glycine residues were added to the peptide in the C-terminal end to link the peptidyl fragment and the ATP mimic. The synthesis (Figure 2C) was accomplished starting from

compound **6**. The *tert*-butyl 3-aminopropylcarbamate was then attached by an amide bond, and the elimination of the Boc protecting group led to compound **11**. The peptide Ac-LNLGG-OH was finally anchored by an amide bond, obtaining the "bidentate" compound **12** in 61% yield.

This compound was subsequently tested against JNK in the kinase activity and pepJIP1 DELFIA displacement assays. Compound **12** showed an IC_{50} of 0.295 μM in the kinase assay in a substrate competitive manner. In addition, the compound also showed an IC_{50} of 0.020 μM in displacing pepJIP1, as measured by the DELFIA assay. This is particularly relevant because the peptide Ac-LNL-OH or the peptide Ac-LNLGG-OH did not show any displacement, up to 200 μM, in the same assay. These data suggest that by tailoring an ATP mimic to a weak docking site binder, it is possible to obtain potent, substrate competitive kinase inhibitors with increased selectivity. In fact, no appreciable inhibitory activity was detected up to 100 μM for compound **12** against the closely related MAPK p38α.

In conclusion, we report here on the synthesis and characterization of the indazole spin-labeled derivative **9** that can be used as a probe for NMR-based second-site screening in proteins of the MAPK family such as JNKs. We demonstrated that this paramagnetic probe is able to detect binders in the substrate docking site of JNK, providing rapid and useful information on the relative orientation of such molecules. This data is critical for the design of bidentate compounds with higher affinity and presumably higher selectivity. We designed and synthesized compound **12** as proof-of-concept in support to this hypothesis, resulting in the first substrate competitive JNK inhibitor with nanomolar activity and no appreciable activity against the most closely related kinase p38α. We are currently working on the use of this probe to detect additional nonpeptide small molecule binders in the JIP1 binding site. Such fragments will be used to synthesize new bidentate compounds, which presumably will have higher affinity, selectivity, and better drug-like properties.

Experimental Section

General

Unless otherwise indicated, all anhydrous solvents were commercially obtained and stored in Sure-Seal bottles under nitrogen. All other reagents and solvents were purchased as the highest grade available and used without further purification. NMR spectra were recorded on Varian 300 or Bruker 600 MHz instruments. Chemical shifts (δ) are reported in parts per million (ppm) referenced to ^{1}H (Me$_4$Si at 0.00). Coupling constants (J) are reported in Hz throughout. Mass spectral data were acquired on an Esquire LC00066 for low resolution, an Agilent ESI-TOF for high resolution, or a JEOL LC-mate tuned for either low resolution or high resolution. Retention time for product **8** was obtained in a HPLC Breeze from Waters Co. using an Atlantis T3 3 μm 4.6 mm × 150 mm reverse phase column. The progress of reactions was monitored by TLC. The purity of the key compounds **9** and **12** was determined by HPLC (Supporting Information), resulting in a purity greater than 95%.

Synthesis of 3-Iodo-1*H*-indazole (3)

The compound **2** (indazole) was commercially available, which was iodinated according to the reported procedures to give product **3**.[28,29]

Synthesis of *tert*-Butyl-3-iodo-1*H*-indazole-1-carboxylate (4)

To a solution of **3** (3.66 g, 15 mmol) in CH$_3$CN (30 mL) were added Et$_3$N (3.13 mL, 22.5 mmol) and DMAP (90 mg, 0.75 mmol, 5 mol%) at room temperature under nitrogen atmosphere. After 10 min, (Boc)$_2$O (3.59 g, 16.5 mmol) was added to the reaction mixture. The resulting reaction mixture was stirred at room temperature for 10 h, then the solvent and triethyl amine were removed in vacuo. The residue was extracted with ether (200 mL), and

washed with brine (2×50 mL), dried ($MgSO_4$), and then concentrated. The residue was chromatographed over silica gel (5% ethyl acetate in hexane) to give the pure product **4** (5.14 g, 92%).

^{1}H NMR (300 MHz, CDCl$_3$) δ: 1.72 (s, 9 H), 7.37 (t, J = 8.1 Hz, 1 H), 7.49 (d, J = 8.1 Hz, 1 H), 7.58 (t, J = 7.5 Hz, 1 H), 8.11 (d, J = 8.7 Hz, 1 H). MS m/z 367 (M + Na)$^+$, 345 (M + H)$^+$, 310, 289, 244, 124, 74, 56. HRMS calcd for $C_{12}H_{14}IN_2O_2$ (M + H) 345.0100, found 345.0095.

Synthesis of *tert*-Butyl-3-(4-(methoxycarbonyl)phenyl)-1*H*-indazole-1-carboxylate (5)

A mixture of **4** (344 mg, 1 mmol), 4-methoxycarbonylphenyl boronic acid (271 mg, 1.5 mmol), Pd(dppf)Cl$_2$ (82 mg, 0.1 mmol), and saturated aqueous Na$_2$CO$_3$ solution (4 mL) in ethanol (1 mL) and toluene (10 mL) was stirred at 80 °C for 12 h. After completion of reaction (TLC), the reaction mixture was extracted with CH$_2$Cl$_2$ (3×50 mL). The combined organic layers were washed with saturated NaHCO$_3$ solution (50 mL), water (50 mL), and brine (50 mL), dried (MgSO$_4$), and concentrated in vacuo. The residue was chromatographed over silica gel (10% ethyl acetate in hexane) to give the pure product **5** (228 mg, 65%).

^{1}H NMR (300 MHz, CDCl$_3$) δ: 1.76 (s, 9 H), 4.97 (s, 3 H), 7.40 (t, J = 7.5 Hz, 1 H), 7.58 (t, J = 8.1 Hz, 1 H), 7.99 (d, J = 8.1 Hz, 1 H), 8.10 (d, J = 8.1 Hz, 2 H), 8.15 = 8.26 (m, 3 H). MS m/z 375 (M + Na)$^+$, 353 (M + H)$^+$, 311, 297, 253, 241, 163, 122, 74, 56. HRMS calcd for $C_{20}H_{21}N_2O_4$ (M + H) 353.1501, found 353.1491.

Synthesis of 4-(1*H*-Indazol-3-yl)benzoic acid (6)

To a solution of compound **5** (400 mg, 1.136 mmol) in THF (5 mL) and methanol (1 mL) was added LiOH solution (272 mg, 11.36 mmol) in water (3 mL). The resulting reaction mixture was stirred at room temperature for 18 h. After completion of the reaction, the reaction mixture was acidified with 3 N HCl and stirred for 2 h to remove the boc-group at the same pot. The reaction mixture was extracted with CH$_2$Cl$_2$ (3×50 mL). The combined organic layers were dried over MgSO$_4$ and concentrated in vacuo. The residue was chromatographed over silica gel (5% methanol in dichloromethane) to afford the acid **6** (242 mg, 90%).

^{1}H NMR (300 MHz, DMSO-d_6) δ: 7.25 (t, J = 7.5 Hz, 1 H), 7.43 (t, J = 6.9 Hz, 1 H), 7.63 (d, J = 8.1 Hz, 1 H), 8.02–8.18 (m, 5 H). MS m/z 239 (M + H)$^+$, 201, 158, 129, 102, 84, 56. HRMS calcd for $C_{14}H_{11}N_2O_2$ (M + H) 239.0821, found 239.0820.

Synthesis of Methyl-4-(4-(1*H*-indazol-3-yl)benzamido)butanoate (7)

To a solution of **6** (170 mg, 0.714 mmol) in DMF (3 mL) were added EDC (163 mg, 0.856 mmol), HOBt (120 mg, 0.0.856 mmol), DIEA (0.38 mL, 2.142 mmol), and amine (121 mg, 0.785 mmol) at room temperature. The resulting reaction mixture was stirred at room temperature for 20 h. The reaction mixture was diluted with water (40 mL) followed by extraction with ethyl acetate (3×40 mL). The combined organic layers were washed with saturated NaHCO$_3$ solution (2×30 mL), water (3×30 mL), and brine (30 mL) successively, dried (MgSO$_4$), and then concentrated in vacuo. The residue was chromatographed over silica gel (60% ethyl acetate in hexane) to give the pure product **7** (151 mg, 62%).

^{1}H NMR (300 MHz, DMSO-d_6) δ: 1.82 (quintet, J = 7.5 Hz, 2 H), 2.39 (t, J = 7.5 Hz, 2 H), 3.31 (q, J = 6 Hz, 2 H), 7.24 (t, J = 7.5 Hz, 1 H), 7.42 (t, J = 6.9 Hz, 1 H), 7.62 (d, J = 8.4 Hz, 1 H), 7.99 (d, J = 8.4 Hz, 2 H), 8.05–8.16 (m, 3 H), 8.58 (t, J = 5.1 Hz, 1 H, NH). MS m/z 360 (M + Na)$^+$, 338 (M + H)$^+$, 266, 221, 186, 175, 102, 49. HRMS calcd for $C_{19}H_{20}N_3O_3$ (M + H) 338.1499, found 338.1505.

Synthesis of 4-(4-(1*H*-Indazol-3-yl)benzamido)butanoic acid (8)

To a solution of compound **7** (140 mg, 0.415 mmol) in THF (3 mL) and methanol (1 mL) was added LiOH solution (102 mg, 4.15 mmol) in water (2 mL). The resulting reaction mixture was stirred at room temperature for 18 h. After completion of the reaction, the reaction mixture was acidified with 3 N HCl followed by extraction with CH_2Cl_2 (3×50 mL). The combined organic layers were dried over $MgSO_4$ and concentrated in vacuo. The residue was chromatographed over silica gel (10% methanol in dichloromethane) to afford the acid **8** (122 mg, 91%).

^{1}H NMR (300 MHz, DMSO-d_6) δ: 1.78 (quintet, $J = 7.2$ Hz, 2 H), 2.30 (t, $J = 7.2$ Hz, 2 H), 3.29 (q, $J = 6$ Hz, 2 H), 7.24 (t, $J = 7.5$ Hz, 1 H), 7.40 (t, $J = 7.8$ Hz, 1 H), 7.62 (d, $J = 8.7$ Hz, 1 H), 7.98 (d, $J = 8.1$ Hz, 2 H), 8.02–8.16 (m, 3 H), 8.56 (t, $J = 5$ Hz, 1 H, NH). MS m/z 346 $(M + Na)^+$, 324 $(M + H)^+$, 221, 186, 130, 83. HRMS calcd for $C_{18}H_{18}N_3O_3$ (M + H) 324.1343, found 324.1351.

Synthesis of *N*-(4-(1-Oxo-2,2,6,6-tetramethylpiperidin-4-ylamino)-4-oxobutyl)-4-(1*H*-indazol-3-yl)benzamide (9)

To a solution of compound **8** (50 mg, 0.15 mmol) in DMF (3 mL) were added EDC (45 mg, 0.23 mmol), HOBt (24 mg, 0.15 mmol), DIEA (0.075 mL, 0.45 mmol), and 4-aminoTEMPO (28 mg, 0.165 mmol) at room temperature. The resulting reaction mixture was stirred at room temperature for 20 h. The reaction mixture was diluted with water (40 mL) followed by extraction with ethyl acetate (3×40 mL). The combined organic layers were washed with saturated $NaHCO_3$ solution (2×30 mL), water (3×30 mL), and brine (30 mL) successively, dried ($MgSO_4$), and then concentrated in vacuo. The residue was treated with dichloromethane, observing the formation of a precipitate. This precipitate was filtered and dried, resulting in the pure product **9** (49 mg, 68%).

^{1}H NMR (after treatment with HCl_{aq} to destroy the radical, 600 MHz, DMSO-d_6) δ: 1.30 (s, 6 H, CH_3), 1.43 (s, 6 H, CH_3), 1.70–1.85 (m, 3.5 H, CH_2), 1.85–1.94 (m, 1.5 H, CH_2), 1.95–2.03 (m, 1.5 H, CH_2), 2.08–2.20 (m, 3.5 H, CH_2), 3.00–3.10 (m, 0.5 H, CH), 3.45–3.55 (m, 0.5 H, CH), 7.22 (dd, $J_1 = 7.3$ Hz, $J_2 = 7.4$ Hz, 1H, CH arom), 7.41 (dd, $J_1 = 7.3$ Hz, $J_2 = 7.7$ Hz, 1H, CH arom), 7.61 (d, $J = 8.3$ Hz, 1H, CH arom), 7.96–8.04 (m, 2H, CH arom), 8.04–8.08 (m, 2H, CH arom), 8.1 (d, $J = 8.1$ Hz, 1H, CH arom), 8.15 (d, $J = 6.7$ Hz, 0.5 H, CONH), 8.48 (d, $J = 5.9$ Hz, 0.5 H, CONH), 8.58–8.64 (m, 0.5 H, CONH), 8.64–8.70 (m, 0.5 H, CONH), 9.34 (ws, 0.5 H, NOH), 9.45 (ws, 0.5 H, NOH). R_T (solvent A: H_2O with 0.1% formic acid; solvent B: ACN with 0.1% formic acid; linear gradient at 1 mL/min from 95% A and 5% B to 5% A and 95% B in 15 min, $\lambda = 220$ nm): 11.65 min. HRMS calcd for $C_{27}H_{36}N_5O_3$ (M + H) 477.2734, found 477.2735.

Synthesis of *tert*-Butyl-3-(4-(1*H*-indazol-3-yl)benzamido)propylcarbamate (10)

To a solution of **6** (155 mg, 0.421 mmol) in DMF (3 mL) were added EDC (96 mg, 0.505 mmol), HOBt (68 mg, 0.505 mmol), DIEA (0.19 mL, 1.052 mmol), and mono-Boc-1,3-diamino propane (82 mg, 0.463 mmol). The reaction mixture was stirred at room temperature for 16 h. The reaction mixture was diluted with water (40 mL), followed by extraction with ethyl acetate (3×40 mL). The combined organic layers were washed with saturated $NaHCO_3$ solution (2×30 mL), water (3×30 mL), and brine (30 mL) successively, dried ($MgSO_4$), and then concentrated in vacuo. The residue was chromatographed over silica gel (50% ethyl acetate in hexane) to give the pure product **10** (175 mg, 79%).

^{1}H NMR (300 MHz, CD_3OD) δ: 1.47 (s, 9 H), 1.87 (quintet, $J = 6.6$ Hz, 2 H), 3.18 (t, $J = 6.6$ Hz, 2 H), 3.48 (t, $J = 6.6$ Hz, 2 H), 7.28 (t, $J = 7.2$ Hz, 1 H), 7.47 (t, $J = 6.9$ Hz, 1 H), 7.61 (d, $J = 8.4$ Hz, 1 H), 8.01 (d, $J = 8.4$ Hz, 2 H), 8.08 (d, $J = 8.4$ Hz, 1 H), 8.10 (d, $J = 8.4$ Hz, 2 H).

EIMS m/z 395 (M + H)$^+$, 339, 295, 221, 83. HRMS calcd for $C_{22}H_{27}N_4O_3$ 395.2078 (M + H), found 395.2077.

Synthesis of *N*-(3-Aminopropyl)-4-(1*H*-indazol-3-yl)benzamide (11)

To a solution of compound **10** (41 mg, 0.104 mmol) in CH_2Cl_2 (2 mL) was added TFA (1 mL). The resulting reaction mixture was stirred at room temperature for 2 h. TFA and dichloromethane were removed in vacuo to give **11**. This compound was used for the next step without further purification.

Synthesis of *N*^{1}-(1-(4-(1*H*-Indazol-3-yl)phenyl)-16-methyl-1,7,10,13-tetraoxo-2,6,9,12-tetraazaheptadecan-14-yl)-2-(2-acetamido-4-ethylpentanamido)succinamide (12)

To a solution of **11** (30 mg, 0.102 mmol) in DMF (2 mL) were added EDC (20 mg, 0.104 mmol), HOBt (14 mg, 0.103 mmol), DIEA (0.5 mL), and Ac-LNLGG-OH (44 mg, 0.085 mmol) at room temperature. The reaction mixture was stirred at 50 °C for 16 h. After completion of reaction, DMF and DIEA were removed in vacuo to give crude reaction mixture. The final product was obtained by HPLC purification (41 mg, 61%).

^{1}H NMR (300 MHz, CD$_3$OD) δ: 0.72–0.88 (m, 12 H), 1.10–1.22 (m, 2 H), 1.40–1.1.46 (m, 2 H), 1.50–1.62 (m, 4 H), 1.74 (quintet, J = 6.3 Hz, 2 H), 1.88 (s, 3 H), 2.56–2.79 (m, 2 H), 3.37 (q, J = 4.8 Hz, 2 H), 3.72–3.89 (m, 4 H), 4.10–4.23 (m, 2 H), 4.52–4.59 (m, 2 H), 7.15 (t, J = 7.5 Hz, 1 H), 7.30–7.41 (m, 2 H), 7.49 (d, J = 8.1 Hz, 1 H), 7.62 (d, J = 7.8 Hz, 1 H, NH), 7.76 (br s, NH), 7.90 (d, J = 8.1 Hz, 2 H), 7.94–8.01 (m, 3 H), 8.48 (br s, NH). EIMS m/z 813 (M + Na)$^+$, 791 (M + H)$^+$, 663, 571, 550, 522, 448, 409, 338, 270, 221, 130, 83. HRMS calcd for $C_{39}H_{55}N_{10}O_8$ (M + H) 791.4199, found 791.4186.

pepJIP1 DELFIA Displacement Assay

To each well of 96-well streptavidin-coated plates (Perkin-Elmer), 100 μL of a 100 ng/mL solution of biotin-labeled pep-JIP1 (Biotin-lc-KRPKRPT-TLNLF, where lc indicates a hydrocarbon chain of 6 methylene groups) was added.

After 1 h incubation and elimination of unbound biotin-pep-JIP1 by 3 washing steps, 87 μL of Eu-labeled anti-GST antibody solution (300 ng/mL; 1.9 nM), 2.5 μL DMSO solution containing test compound, and 10 μL solution of GST-JNK2 for a final protein concentration of 10 nM was added. After 1 h incubation at 0 °C, each well was washed 5 times to eliminate unbound protein and the Eu-antibody if displaced by a test compound. Subsequently, 200 μL of enhancement solution (Perkin-Elmer) was added to each well and fluorescence measured after 10 min incubation (excitation wavelength, 340 nm; emission wavelength, 615 nm). Note that measurements are made in time-resolved mode given the relaxation properties of Eu. Controls include unlabeled peptide and blanks receiving no compounds. Protein and peptide solutions were prepared in DELFIA buffer (Perkin-Elmer).

JNK Kinase Activity Assay

The kinase assay was performed based on the LanthaScreen platform from Invitrogen using a time-resolved fluorescence resonance energy transfer assay (TR-FRET) in 384 well plates. Each well received JNK1 (35 ng/mL), ATF2 (400 nM), and ATP (0.2 mM) in 50 mM HEPES, 10 mM MgCl 2, 1 mM EGTA and 0.01% Brij-35, pH 7.5, and test compounds. The kinase reaction was performed at room temperature for 1 h. After this time, the terbium-labeled antiphospho-ATF2 antibody and EDTA were added into each well. After an additional hour incubation, the signal was measured at 520/495 nm emission ratio on a fluorescence plate reader (Victor 2, Perkin-Elmer).

Modeling Studies

Docking studies were performed with GOLD30[-32] and analyzed with Sybyl (Tripos, St. Louis). Molecular surfaces were generated with MOLCAD.[33] The X-ray coordinates of JNK1/pepJIP1/compound **1**, PDB-ID 1UKI, were used to dock the compounds. Molecular models were generated with CON-CORD[34] and energy minimized with Sybyl. For each compound, 10 solutions were generated and subsequently ranked according to Chemscore.[32] Top solutions were used to represent the docked geometry of the azaindole derivative. Peptide poses reported in Figures 1 and 2 of the manuscript correspond to those obtained directly from the X-ray coordinates.

K_i Determination

The paramagnetic compound **9** can also be used as a tool for IC_{50} determination for a given compound in the JIP site when compared against a reference molecule. This is shown in the NMR data obtained for peptide Ac-RPTTLNL-OH when titrated with a JIP-mimic compound BI78D3 (Figure S1, Supporting Information).[35] Because the peptide is being displaced from JNK upon titration of BI78D3, its signals become less affected by the paramagnetic probe **9**. These changes can finally provide an IC_{50} value for BI78D3.

We can also determinate the K_i for compound BI78D3 employing the Cheng–Prusoff equation (Figure S2, Supporting Information).[36] Accordingly, with this equation, our experimental NMR data estimates that the K_i for compound BI78D3 against JNK is 1.3 μM. This data is in agreement of that obtained previously in our laboratory.[35]

Supplementary Material

Refer to Web version on PubMed Central for supplementary material.

Acknowledgments

References

(1). Manning AM, Davis RJ. Targeting JNK for therapeutic benefit: from junk to gold. Nature Rev 2003;2:554–565.

(2). Manning AM, Mercurio F. Transcription inhibitors in inflammation. Exp. Opin. Invest. Drugs 1997;6:555–567.

(3). Gum R, Wang H, Lengyel E, Juarez J, Boyd D. Regulation of 92 kDa type IV collagenase expression by the jun aminoterminal kinase and the extracellular signal-regulated kinase-dependent signaling cascades. Oncogene 1997;14:1481–1493. [PubMed: 9136992]

(4). Xia Z, Dickens M, Raingeaud J, Davis RJ, Greenberg ME. Opposing effects of ERK and JNK-p38 MAP kinases on apoptosis. Science 1995;270:1326–1331. [PubMed: 7481820]

(5). Le-Niculescu H, Bonfoco E, Kasuya Y, Claret F-X, Green DR, Karin M. Withdrawal of survival factors results in activation of the JNK pathway in neuronal cells leading to Fas ligand induction and cell death. Mol. Cell. Biol 1999;19:751–763. [PubMed: 9858598]

(6). Lee YH, Giraud J, Davis RJ, White MF. c-Jun N-terminal kinase (JNK) mediates feedback inhibition of the insulin signaling cascade. J. Biol. Chem 2003;278:2896–2902. [PubMed: 12417588]

(7). Standaert ML, Bandyopadhyay G, Galloway L, Soto J, Ono Y, Kikkawa U, Farese RV, Leitges M. Effects of knockout of the protein kinase C β gene on glucose transport and glucose homeostasis. Endocrinology 1999;140:4470–4477. [PubMed: 10499500]

(8). Ip YT, Davis RJ. Signal transduction by the c-Jun N-terminal kinase (JNK): from inflammation to development. Curr. Opin. Cell Biol 1998;10:205–219. [PubMed: 9561845]

(9). Potapova O, Haghighi A, Bost F, Liu C, Birrer MJ, Gjerset R, Mercola D. The Jun kinase/stress-activated protein kinase pathway functions to regulate DNA repair and inhibition of the pathway sensitizes tumor cells to cisplatin. J. Biol. Chem 1997;272:14041–14044. [PubMed: 9162025]

(10). Potapova O, Gorospe M, Bost F, Dean NM, Gaarde WA, Mercola D, Holbrook NJ. c-Jun N-terminal kinase is essential for growth of human T98G glioblastoma cells. J. Biol. Chem 2000;275:24767–24775. [PubMed: 10825181]

(11). Kallunki T, Deng T, Hibi M, Karim M. c-Jun can recruit JNK to phosphorylate dimerization partners via specific docking interactions. Cell 1996;87:929–939. [PubMed: 8945519]

(12). Yang SH, Whitmarsh AJ, Davis RJ, Sharrocks A. Differential Targeting of MAP kinases to the ETS-domain transcription factor Elk-1. EMBO J 1998;17:1740–1749. [PubMed: 9501095]

(13). Whitmarsh AJ, Cavanagh J, Tournier C, Yasuda J, Davis RJ. A mammalian scaffold complex that selectively mediates MAP kinase activation. Science 1998;281:1671–1674. [PubMed: 9733513]

(14). Dickens M, Roger JS, Cavanagh J, Raitano A, Xia Z, Halpern JR, Greenberg ME, Sawyer CL, Davis RJ. A cytoplasmic inhibitor of the JNK signal transduction pathway. Science 1997;277:693–696. [PubMed: 9235893]

(15). Bonny C, Oberson A, Negri S, Sauser C, Schorderet DF. Cell-permeable peptide inhibitors of JNK: novel blockers of beta-cell death. Diabetes 2001;50:77–82. [PubMed: 11147798]

(16). Barr RK, Kendrick TS, Bogoyevitch MA. Identification of the critical features of a small peptide inhibitor of JNK activity. J. Biol. Chem 2002;277:10987–10997. [PubMed: 11790767]

(17). Bennett BL, Sasaki DT, Murray BW, O'Leary EC, Sakata ST, Xu W, Leisten JC, Motiwala A, Pierce S, Satoh Y, Bhagwat SS, Manning AM, Anderson DW. SP600125, an anthrapyrazolone inhibitor of Jun N-terminal kinase. Proc. Natl. Acad. Sci. U.S.A 2001;98:13681–13686. [PubMed: 11717429]

(18). Heo YS, Kim S-K, Seo CI, Kim YK, Sung B-J, Lee HS, Lee JI, Park S-Y, Kim JH, Hwang KY, Hyun Y-L, Jeon YH, Ro S, Cho JM, Lee TG, Yang C-H. Structural basis for the selective inhibition of JNK1 by the scaffolding protein JIP and SP600125. EMBO J 2004;23:2185–2195. [PubMed: 15141161]

(19). Jahnke W. Spin labels as a tool to identify and characterize protein–ligand interactions by NMR spectroscopy. ChemBioChem 2002;3:167–173. [PubMed: 11921394]

(20). Jahnke W, Floersheim P, Ostermeier C, Zhang X, Hemmig R, Hurth K, Uzunov DP. NMR reporter screening for the detection of high-affinity ligands. Angew. Chem., Int. Ed 2002;41:3420–3423.

(21). Jahnke W, Blommers MJJ, Fernandez C, Zwingelstein C, Amstutz R. Strategies for the NMR-based identification and optimization of allosteric protein kinase inhibitors. ChemBioChem 2005;6:1607–1610. [PubMed: 16028302]

(22). Vazquez J, Tautz L, Ryan JJ, Vuori K, Mustelin T, Pellecchia M. Development of molecular probes for second-site screening and design of protein tyrosine phosphatase inhibitors. J. Med. Chem 2007;50:2137–2143. [PubMed: 17394300]

(23). Dalvit C, Flocco M, Knapp S, Mostardini M, Perego R, Stockman BJ, Veronesi M, Vasari M. High-throughput NMR-based screening with competition binding experiments. J. Am. Chem. Soc 2002;124:7702–7709. [PubMed: 12083923]

(24). Shuker SB, Hajduk PJ, Meadows RP, Fesik SW. Discovering high-affinity ligands for proteins: SAR by NMR. Science 1996;274:1531–1534. [PubMed: 8929414]

(25). Becattini B, Sareth S, Zhai D, Crowell KJ, Leone M, Reed JC, Pellecchia M. Targeting apoptosis via chemical design: inhibition of bid-induced cell death by small organic molecules. Chem. Biol 2004;11:1107–1117. [PubMed: 15324812]

(26). Becattini B, Pellecchia M. SAR by ILOEs: an NMR-based approach to reverse chemical genetics. Chem.sEur. J 2006;12:2658–2662.

(27). Chen J, Zhang Z, Stebbins JL, Zhang X, Hoffman R, Moore A, Pellecchia M. A fragment-based approach for the discovery of isoform-specific p38alpha inhibitors. ACS Chem. Biol 2007;2:329–336. [PubMed: 17465519]

(28). Collot V, Dallemagne P, Bovy PR, Rault S. Suzuki-type cross-coupling reaction of 3-iodoindazoles with aryl boronic acids: A general and flexible route to 3-arylindazoles. Tetrahedron 1999;55:6917–6922.

(29). Collot V, Bovy PR, Rault S. Heck cross-coupling reaction of 3-iodoindazoles with methyl acrylate: a mild and flexible strategy to design 2-aza tryptamines. Tetrahedron Lett 2000;41:4363–4366.

(30). *Gold*, version 2.1. The Cambridge Crystallographic Data Centre; 12 Union Road, Cambridge CB2 1EZ, UK:

(31). Jones G, Willett P, Glen RC, Leach AR, Taylor R. Development and validation of a genetic algorithm for flexible docking. J. Mol. Biol 1997;267:727–748. [PubMed: 9126849]

(32). Eldridge MD, Murray CW, Auton TR, Paolini GV, Mee RP. Empirical scoring functions: I. The development of a fast empirical scoring function to estimate the binding affinity of ligands in receptor complexes. J. Comput.-Aided Mol. Des 1997;11:425–445. [PubMed: 9385547]

(33). Teschner M, Henn C, Vollhardt H, Reiling S, Brickmann J. Texture mapping: A new tool for molecular graphics. J. Mol. Graphics 1994;12:98–105.

(34). Pearlman, RS. Concord. Concord; St. Louis, MO: 1998. distributed by Tripos

(35). Stebbins JL, De SK, Machleidt T, Becattini B, Vazquez J, Kuntzen C, Chen L-H, Riel-Mehan M, Emdadi A, Solinas G, Karin M, Pellecchia M. Identification of a novel JNK inhibitor targeting JNK-JIP interaction site. Nature. 2007 submitted for publication.

(36). Cheng Y, Prusoff WH. Relationship between the inhibition constant (K_i) and the concentration of inhibitor which causes 50% inhibition (IC_{50}) of an enzymatic reaction. Biochem. Pharmacol 1973;22:3099–3108. [PubMed: 4202581]
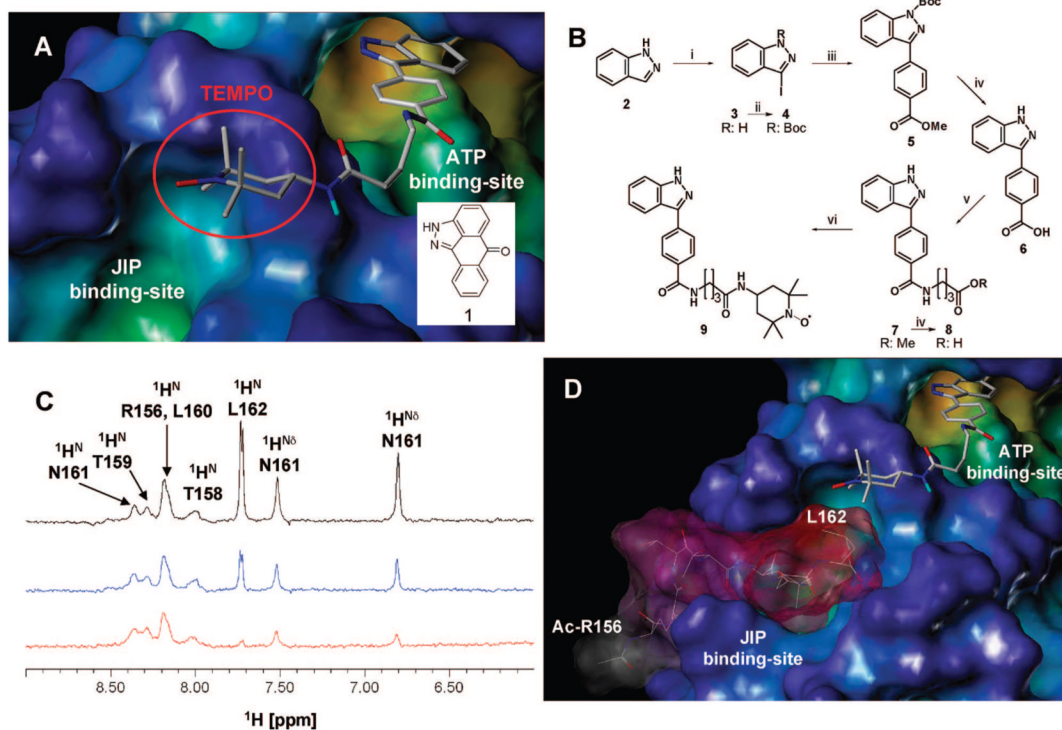
Figure 1.
(A) Docking of compound **9** in JNK. The surface of the protein is displayed to show the cavities and the compound is displayed in capped sticks without protons to better visualize its structure. The chemical structure of **1** is also reported. (B) Synthesis of the paramagnetic probe **9**: (i) I_2, KOH, DMF, 1 h, r.t.; (ii) Boc_2O, DMAP, CH_3CN, 10 h, r.t.; (iii) 4-methoxycarbonylphenyl boronic acid, Pd(dppf)Cl_2, Na_2CO_3, toluene/ethanol (10:1), 12 h, 80 °C; (iv) LiOH, THF/MeOH (5:1), 18 h, r.t.; (v) methyl 4-aminobutanoate, EDC, HOBt, DIEA, DMF, 20 h, r.t; (vi) 4-aminoTEMPO, EDC, HOBt, DIEA, DMF, 20 h, r.t.. (C) Amide region of $T_{1\rho}$ experiments (100 ms spin lock time) of peptide Ac-RPTTLNL-OH (1 mM) in the presence of 200 μM compound **9** (black), in the presence of 10 μM of protein JNK (blue), and in the presence of both 200 μM of compound **9**, and 10 μM of protein JNK (red). (D) Docking of compound **9** and peptide Ac-RPTTLNL-OH in JNK. The surface of the protein is displayed to highlight the cavities, the compound is displayed in capped sticks without protons to better visualize the structure and the peptide is displayed in sticks with a translucent surface in a gradient from red to grey coding for the effect of the paramagnetic probe in each residue: red, more affected; grey, less affected. Peptide pose correspond to that obtained directly from the X-ray structure PDB-ID 1UKI.
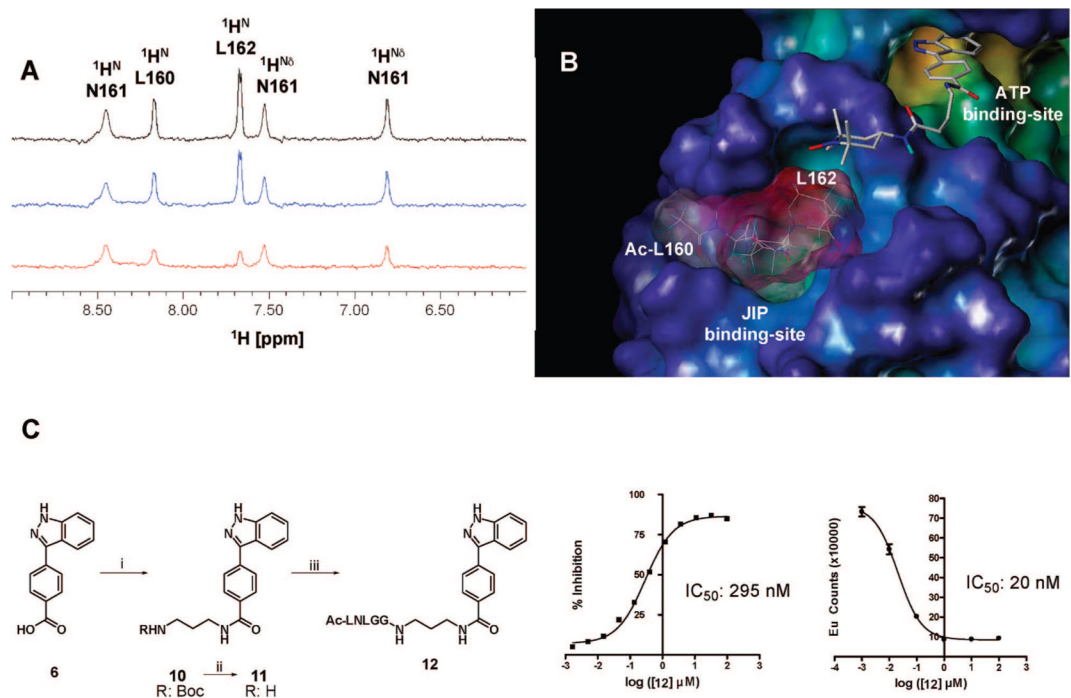
Figure 2.
(A) Amide region of $T_{1\rho}$ experiments (100 ms spin lock time) of peptide Ac-LNL-OH (1 mM) in the presence of 200 μM compound **9** (black), in th epresence of 10 μM of protein JNK (blue), and in the presence of both 200 μM of compound **9** and 10 μM of protein JNK (red). (B) Docking of compound **9** and peptide Ac-LNL-OH in JNK. The surface of the protein is displayed to highlight the cavities, the compound is displayed in capped sticks without protons to better visualize the structure, and the peptide is displayed in sticks with a translucent surface in a gradient from red to grey coding for the effect of the paramagnetic probe in each residue: red, more affected; grey, less affected. Peptide pose correspond to that obtained directly from the X-ray structure PDB-ID 1UKI. (C) Synthesis of the bidentate compound **12**: (i) *tert*-butyl 3-aminopropylcarbamate, EDC, HOBt, DIEA, DMF, 16 h, r.t.; (ii) TFA/DCM (1:1), 2 h, r.t.; (iii) Ac-LNLGG-OH, EDC, HOBt, DIEA, DMF, 16 h, 50 °C; (D) IC$_{50}$ curves obtained for compound **12** in the kinase assay (left) and in the DELFIA displacement assay (right).